Materials Research, Vol. 6, No. 1, 43-45, 2002.

Spectroscopy Studies of 4H-SiC

A.C. de Oliveira[a]*, *J.A. Freitas Jr.*[b], *W.J. Moore*[b], *A. Ferreira da Silva*[c], *I. Pepe*[c,d], *J. Souza de Almeida*[c,e], *J.M. Osório-Guillén*[f], *R. Ahuja*[f], *C. Persson*[f], *K. Järrendahl*[g], *O.P.A. Lindquist*[g], *N.V. Edwards*[g,h], *Q. Wahab*[g]

[a]*Instituto de Física, Universidade de Brasília, 70919-970, Brasília - DF, Brazil*
[b]*Naval Research Laboratory, Washington, D.C. 20375, USA*
[c]*Instituto de Física, Universidade Federal da Bahia, 40210-340, Salvador - Ba, Brazil*
[d]*LPCC, College de France, F-75231 Paris, France*
[e]*DCC, Faculdade Ruy Barbosa, 41940-320 Salvador - Ba, Brazil*
[f]*Department of Physics, Uppsala University, SE-75121 Uppsala, Sweden*
[g]*Department of Physics, Linköping University, SE-58183 Linköping, Sweden*
[h]*Motorola Semiconductor Products, 2200 West Broadway Road, Mesa AZ 85202 USA*

Received: January 02, 2002; Revised: September 30, 2002

Calculations of the total dielectric functions and the optical bandgap energy (OBGE) of 4H-SiC were performed by the full-potential linear muffin-tin-orbital method. The results are compared to spectroscopic ellipsometry dielectric measurements agreeing closely over in a wide range of energies. The obtained theoretical value of the (OBGE) agrees very closely with the measured ones obtained by transmission and photoacoustic spectroscopies at room temperature performed on 470 μm thick wafer and a 25 μm thick homoepitaxial layer of 4H-SiC samples grown (n-type, Si-face) by hot wall CVD.

Keyword: *optical bandgap energy, wide-bandgap material, SiC polytypes, computer simulation*

1. Introduction

The physical properties of the large bandgap 4H-SiC make it a prominent material for high-power, high-temperature, and high-frequency devices. Devices like field effect transistors, bipolar storage capacitors, and ultraviolet detectors have been fabricated[1,2,3].

In this work, we have investigated the optical properties of undoped and *n*-type 4H-SiC, both experimentally and theoretically. The transmission and photoacoustic spectroscopy techniques have been used for the measurement of the optical bandgap energy[3-5]. The total dielectric functions were determined by spectroscopic ellipsometry (SE), a powerful non-destructive technique for high accuracy measurements[5-7]. The calculations of the total dielectric functions were performed by the full-potential linear muffin-tin-orbital method[5,8].

2. Experimental Details

The experimental transmission and photoacoustic spectroscopy apparatus consists of a halogen lamp used as the light source for the measurement. The polychromatic beam is diffracted by a plane diffraction gratings attached to a step-motor. The beam can be varied from 925 to 360 nm, a set of lens and collimator produces a monochromatic light focused onto the sample, see Refs. 3-5.

3. Calculation of the Dieletric Function

The dielectric function was calculated in the momentum representation, which requires matrix elements of the momentum, **p**, between occupied and unoccupied eigenstates. To be specific the imaginary part of the dielectric function, $\varepsilon_2(\omega) = \mathrm{Im}\varepsilon(\mathbf{q} = \mathbf{0},\omega)$, was calculated from[5]

$$\varepsilon_2^{ij}(\omega) = \frac{4\pi^2 e^2}{\Omega m^2 \omega^2} \sum_{\mathbf{k}nn'\sigma} \langle \mathbf{k}n\sigma | p_i | \mathbf{k}n'\sigma \rangle \langle \mathbf{k}n'\sigma | p_j | \mathbf{k}n\sigma \rangle \times$$

$$\times f_{\mathbf{k}n}(1 - f_{\mathbf{k}n'}) \delta(e_{\mathbf{k}n'} - e_{\mathbf{k}n} - \eta\omega) \qquad (1)$$

*e-mail: aderbal@unb.br

In Eq. 1, *e* is the electron charge, *m* its mass, W is the crystal volume and $f_{\mathbf{k}n}$ is the Fermi distribution. Moreover, $|\mathbf{k}n\sigma\rangle$ is the crystal wave function corresponding to the nth eigenvalue with crystal momentum **k** and spin s.

With our spherical wave basis functions, the matrix elements of the momentum operator are conveniently calculated in spherical coordinates and for this reason the momentum is written $\mathbf{p} = \sum_\mu e^*_\mu p_\mu$, where *m* is -1, 0, or 1, and

$p_{-1} = \frac{1}{\sqrt{2}}(p_x - ip_y)$, $p_0 = p_z$, and $p_1 = \frac{-1}{\sqrt{2}}(p_x - ip_y)$ [2,3].

The evaluation of the matrix elements in Eq. 2 is done over the muffin-tin region and the interstitial separately[5]. A full detailed description of the calculation of the matrix elements was presented somewhere else[9]. In our theoretical method the wave function [Eq. 1] inside the muffin-tin spheres is atomic-like in the sense that it is expressed as a radial component times spherical harmonic functions (also involving the so called structure constants), i.e.,

$$\Psi^{\bar{k}}_{mt}(\bar{r}) = \sum_t c_t \chi^{\bar{k}}_t , \qquad (2)$$

where inside the sphere *R*' the basis function is

$$\chi^{\bar{k}}_t = \frac{\Phi_t(\bar{r}-\bar{R})}{\Phi(S^R_{mt})}\delta_{\bar{R},R'} - \sum_{t'}\frac{\Phi_{t'}(\bar{r}-\bar{R}')}{\Phi(S^{R'}_{mt})}S^{\bar{k}}_{t,t'}, \qquad (3)$$

and

$$\Phi_t(\bar{r}) = i^l Y^m_l(\hat{r})(\varphi(r) + \omega(D)\dot{\varphi}(r)) \qquad (4)$$

In the equations above S^R_{mt} is the muffin-tin radius for atom R, $S^{\bar{k}}_{tt'}$ is the structure constant, *D* is the logarithmic derivative, $\varphi(r)$ is the numerical solution to the spherical component of the muffin-tin potential and $\dot{\varphi}(r)$ is the energy derivative of $\varphi(r)$. Therefore, this part of the problem is quite analogous to the atomic sphere approximation (ASA) calculations and we calculate the matrix elements in Eq. 2 as[5]

$$\langle \mathbf{k}n\sigma | p_i | \mathbf{k}n'\sigma \rangle = \sum_{t,t'} c_t c^*_{t'} \langle x_{t'} | p_\mu | x_t \rangle \qquad (5)$$

Since, χ_t involves a radial function multiplied with a spherical harmonic function, i.e., $f(r)Y_l^m$ (we will label this product $|l,m\rangle$), we can calculate the matrix elements in Eq. 5 using the relations

$$\langle l+1,0|p_0|l,0\rangle = \frac{l+1}{\sqrt{(2l+1)(2l+3)}}\left\langle f^*(r)\left(\frac{\delta}{\delta r} - \frac{l}{r}\right)f(r)\right\rangle, \qquad (6)$$

and

$$\langle l-1,0|p_0|l,0\rangle = \frac{l+1}{\sqrt{(2l-1)(2l+1)}}\left\langle f^*(r)\left(\frac{\delta}{\delta r} - \frac{l+1}{r}\right)f(r)\right\rangle, \qquad (7)$$

A general matrix element, $\langle l',m'|p_i|l,m\rangle$, is then calculated using the Wigner-Eckart theorem[5]. Matrix elements of the momentum over the interstitial are obtained from the relation

$$\int_{\Omega_{\text{int}}} d^3r\left(\psi^*_i \vec{\nabla}\psi_j\right) = \frac{1}{k_j^2}\int_{\Omega_{\text{int}}} d^3r\left(\psi^*_i \nabla^2 \vec{\nabla}\psi_j\right). \qquad (8)$$

By use of Green's second theorem the expression above can be expressed as

$$\int_{\Omega_{\text{int}}} d^3r\left(\psi^*_i \nabla^2 \vec{\nabla}\psi_j\right) = -\int_{S_{MT}} dS\left(\psi^*_i \vec{\nabla}\frac{d}{dr}\psi_j\right). \qquad (9)$$

In the expression above the surface integral is taken over the muffin-tin spheres and since the interstitial wave function by construction is the same as the muffin-tin wave function we can use for ψ the numerical wave function defined inside (and on the boundary of) the muffin-tin spheres. In this way the evaluation of the integral above is done in a quite similar way as done for the muffin-tin contribution [Eqs. 6-8] to the gradient matrix elements.

The summation over the Brillouin zone in Eq. 1 is calculated using linear interpolation on a mesh of uniformly distributed points, i.e., the tetrahedron method. The matrix elements, eigenvalues and eigenvectors are calculated in the irreducible part of the Brillouin-zone.

The correct symmetry for the dielectric constant was obtained by averaging the calculated dielectric function. Finally, the real part of the dielectric function, $\varepsilon_1(\omega)$, is obtained from $\varepsilon_2(\omega)$ using the Kramers-Kronig transformation,

$\varepsilon_1(\omega)$ º Re($\varepsilon(\mathbf{q}=0,\omega)$) =

$$1 + \frac{1}{\pi}\int_0^\infty d\omega' \varepsilon_2(\omega')\left(\frac{1}{\omega'-\omega} + \frac{1}{\omega'+\omega}\right). \qquad (10)$$

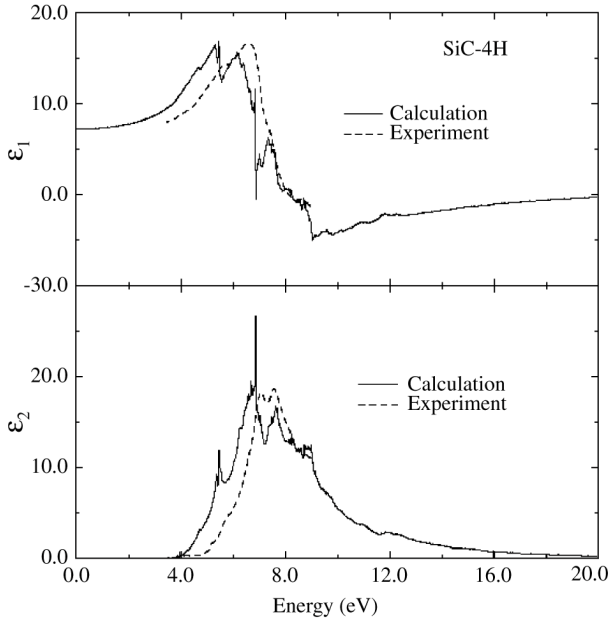

Figure 1. The total real part e_1 and imaginary part e_2 of the dielectric functions.

Table 1. Obtained values of the bandgap energies E_g of 4H-SiC using photoacoustic (PA) and transmission (TR) measurements and theoretical (Theory) calculation.

	PA	TR	TR n-type	Theory
4H-SiC	3.30± 0.02	3.30± 0.02	3.26± 0.01	3.40± 0.01

The total average dielectric functions are given by

$$\varepsilon_{1,2}(\omega) = \frac{\varepsilon_{1,2}^{\parallel}(\omega) + 2\varepsilon_{1,2}^{\perp}(\omega)}{3} \qquad (11)$$

4. Results

The values of the optical bandgap energies are shown in Table 1. They are very close when compared to different measurements as well as to the theoretical result. From the electronic structure and the partial density of states we can identify the optical absorption described by the imaginary part of the dielectric function and then obtain the bandgap energy[5]. The measured total dielectric functions, ε_1 and ε_2 are shown in Fig. 1 together with the theoretical results. There is a good agreement between the measured and the calculated dielectric functions.

5. Conclusion

We have measured the optical properties of 4H-SiC, using transmission and photoacoustic spectroscopies and spectroscopic ellipsometry. The resulting total dielectric functions and optical bandgap energies are in excellent agreement with our full-potential calculations. By comparing the total dielectric functions we conclude that the optical anisotropy is small in 4H-SiC.

Acknowledgements

This work was financially supported by: the Swedish agencies TFR, NFR and SSF, Brazilian agencies CNPq and FAP-DF, and at the Naval Research Laboratory by the Office of Naval Research.

Reference

1. Morkoc, H.; Strite, S.; Gao, G.B.; Lin, M.E.; Sverdlov, B.; Burns, M. *J. Appl. Phys.*, v. 76, p. 1363, 1994.
2. Palmour, J.W.; Edmond, J.A.; Kong, H.S.; Carter Jr., C.H. *Physica B*, v. 185, p. 461, 1993.
3. Oliveira, A.C.; Freitas Jr., J.A.; W.J. Moore (to appear).
4. Silva, A.F.; Veissid, N.; An, C.Y.; Pepe, I.; Oliveira, N.B.; Silva, A.V.B. *Appl. Phys. Lett.*, v. 69, p. 1930, 1996.
5. Ahuja, R.; Silva, A.F.; Persson, C.; Osorio-Guillén, J.M.; Pepe, I.; Järrendahl, K.; Lindquist, O.P.A.; Edwards, N.V.; Wahab, Q.; Johansson, B. *J. Appl. Phys.* (in press).
6. S. Zangooie, P.O.A. Persson, J.N. Hilfiker, L. Hultman, H. Arwin *J. Appl. Phys.*, v. 87, p. 8497, 2000.
7. Lindquist, O.P.A; K. J\"{a}rrendahl, Peters, S.; Zettler, J.-T.; Cobet, C.; Esser, N.; Aspnes, D.E. *Appl. Phys. Lett.*, v. 78, p. 2751, 2001.
8. Wills, J.M.; (unpublished); Wills, J.M.; Cooper, B.R. *Phys. Rev. B*, v. 36, p. 3809, 1987; Price, D.L.; Cooper, B.R. *ibid.*, v. 39, p. 4945, 1989.
9. Ahuja, R.; Auluck, S.; Wills, J.M.; Alouani, M.; Johansson, B.; Eriksson, O. *Phys. Rev. B*, v. 55, p. 4999, 1997.
10. A good description of the calculation of dielectric constants and related properties is found in the thesis by T. Gashe, Uppsala University, 1993.